AGU Word Manuscript Template

Climate-induced Severe Water Scarcity Events as Harbingers of Global Wheat Price

Miroslav Trnka[1,2], Jan Meitner [1,2], Jan Balek[1,2], Song Feng[3], Juliana Arbelaez Gaviria [1,2,4], Milan Fischer[1,2], Esther Boere[4,5], Petr Havlík[4], Kurt-Christian Kersebaum[1,6,7], Claas Nendel[6,8], Margarita Ruiz-Ramos[9], Daniela Semerádová[1,2], Mikhail A. Semenov [10], Markéta Poděbradská[1,2], Jan Esper[1,11], Ulf Büntgen[1,12, 13], Max Torbenson[11], Jáchym Brzezina[1], Zdeněk Žalud[1,2], Gabriel Katul[14,1], Jørgen E. Olesen[1,15,16]

[1]*Global Change Research Institute CAS, Bělidla 986/4b, Brno, 603 00, Czech Republic, +420 725 950 927; mirek_trnka@yahoo.com*

[2]*Department of Agrosystems and Bioclimatology, Mendel University in Brno, Zemědělská 1, Brno 613 00, Czech Republic*

[3]Department of Geosciences, University of Arkansas, Fayetteville, Arkansas, USA, +1 479-575-4748

[4]*International Institute for Applied Systems Analysis (IIASA), Schlossplatz 1, A-2361 Laxenburg, Austria*

[5] *Vrije Universiteit, VU University Amsterdam, De Boelelaan 1085, 1081 HV Amsterdam, The Netherlands*

[6]*Leibniz Centre for Agricultural Landscape Research (ZALF), Müncheberg, Germany*

[7]*Georg August University, Göttingen, Germany*

[8]*University of Potsdam, Institute of Biochemistry and Biology, Potsdam, Germany*

[9]*CEIGRAM-Research Centre for the Management of Agricultural and Environmental Risks, Universidad Politécnica de Madrid, Senda del Rey 13, 28040 Madrid, Spain*

[10]Rothamsted Research, Harpenden, Herts, AL5 2JQ, UK

[11]Department of Geography, Johannes Gutenberg University, Becherweg 21, 55099 Mainz, Germany

[12]Department of Geography, University of Cambridge, Downing Place, CB2 3EN, UK, +44 1223 760564

[13]Swiss Federal Research Institute WSL, Zürcherstrasse 111, 8903 Birmensdorf, Switzerland

[14] Department of Civil and Environmental Engineering, Duke University, 121 Hudson Hall, Box 90287, Durham, NC 27708-0287, USA

[15]Department of Agroecology, Aarhus University, Blichers Allé 20, 8830 Tjele, Denmark, +45 40821659

[16]iCLIMATE Interdisciplinary Centre for Climate Change, Aarhus University, Frederiksborgvej 399, 4000 Roskilde, Denmark

Corresponding author: Miroslav Trnka (trnka.m@czechglobe.cz)

Figs. S1 to S9 & Tables S1 to S4

Open data: All data used in the final analyses are stored in the ASEP data repository of the Czech Academy of Sciences (https://doi.org/10.57680/asep.0638995)

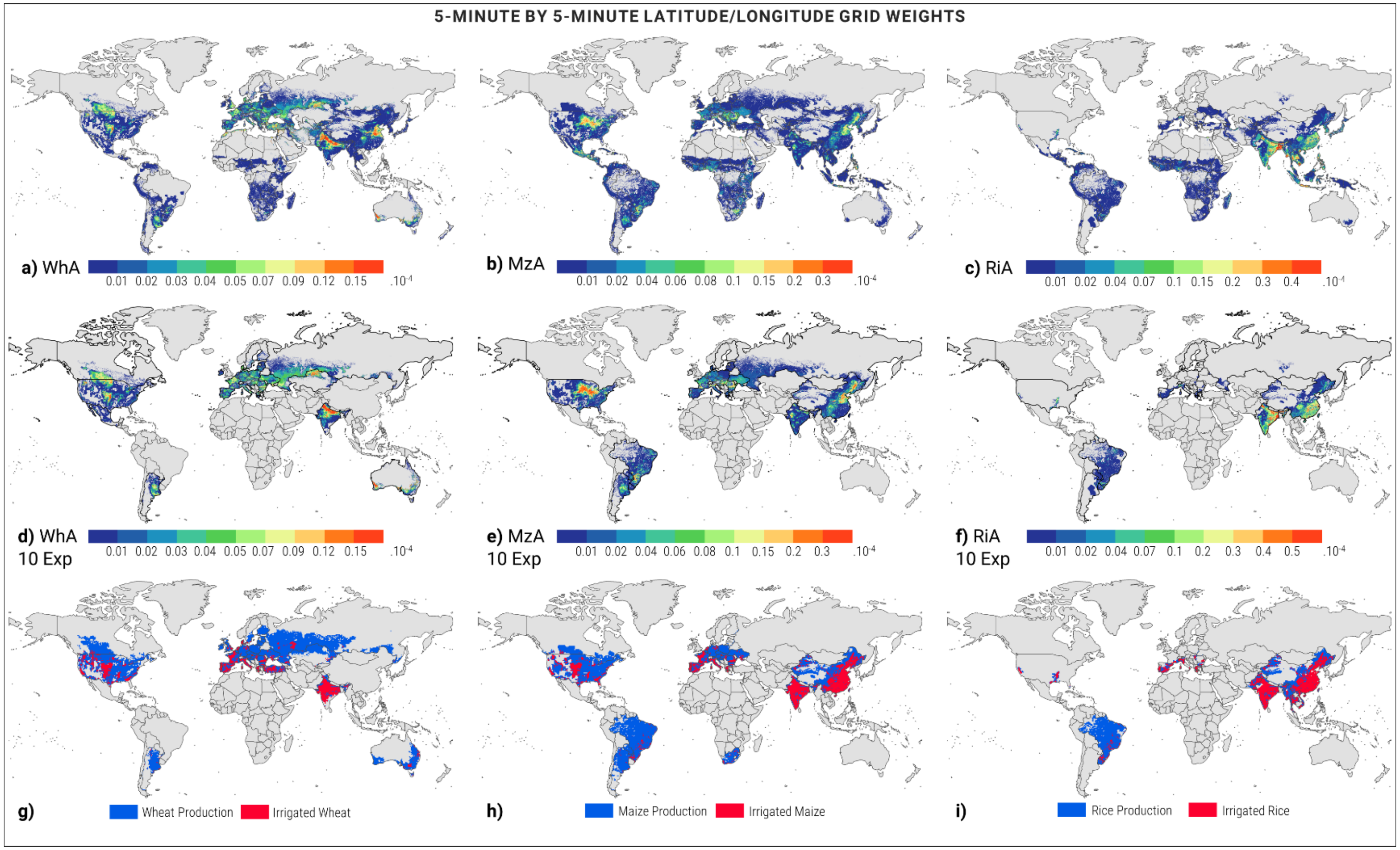

Fig. S1. Weights of the grids used in this study. a-c) Wheat, maize and rice grids: Grids where the given crop is grown, based on Monfreda *et al.* (2008) and Ramankutty *et al*. (2008), with the weights based on the overall proportion of arable land; d-f) the weights were assigned based on the share of the wheat-, maize- and rice-growing area in the grid in relation to the crop-growing area of the top ten exporters; g-i) indication of the main producing areas and potentially irrigated area of the given crop.

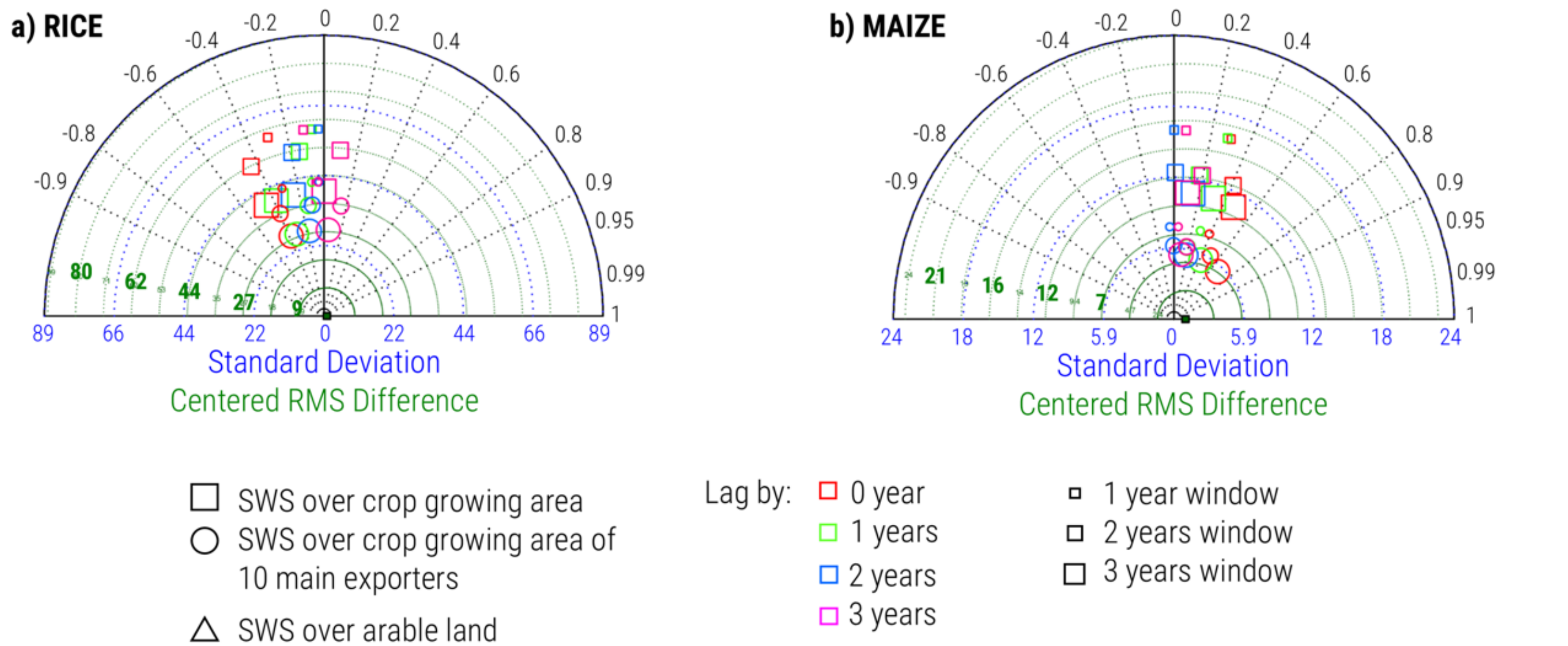

Fig. S2. Results of the fit of severe water scarcity (SWS) and the Wheat Price to form crop price models in the form of Taylor diagrams for (a) rice and (b) maize, where different areas, lags (0–3 years) and time windows (1–3 years) of SWS are considered. The diagram visualizes the Pearson correlation coefficient and standard deviation. The black dot indicates the perfect fit (model with a Pearson correlation coefficient r=1 and a root-mean squared error (RMSE)=0) and the cros the performance of the model ensemble;

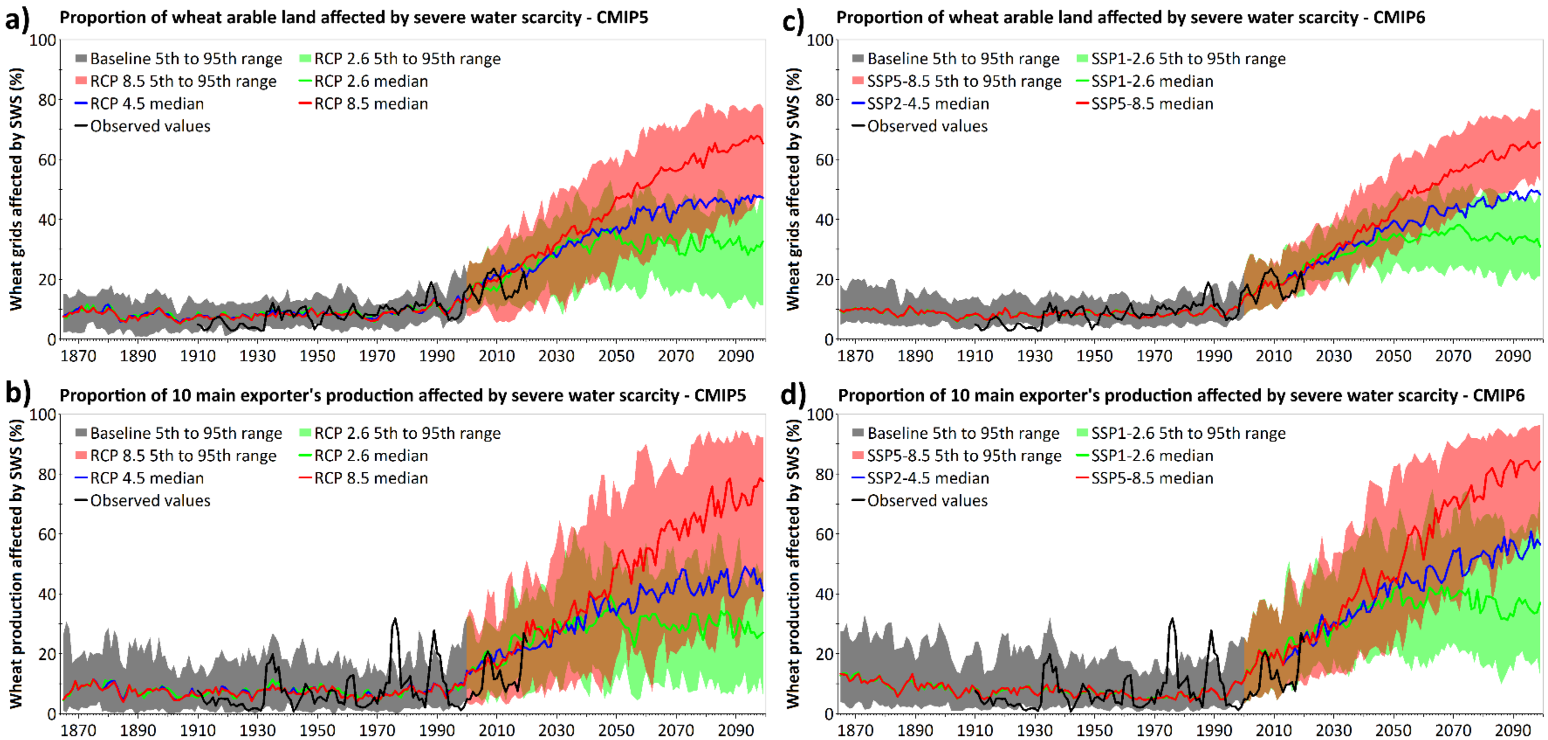

Fig. S3. Time series of severe water scarcity (SWS) for the entire wheat-growing area (a, c) and area of wheat cultivation of the top 10 wheat exporters (b-d) for the baseline climate and projections based on the CMIP5 (a, b) and CMIP6 (c, d) GCM models.

a) Arable

Lag \ Window	1 RMSE	1 R2	2 RMSE	2 R2	3 RMSE	3 R2
0	46	0.01	42	0.19	41	0.20
1	41	0.23	29	0.62	34	0.49
2	37	0.40	33	0.51	27	0.68
3	43	0.19	41	0.24	35	0.46

b) WhA10Ex

Lag \ Window	1 RMSE	1 R2	2 RMSE	2 R2	3 RMSE	3 R2
0	44	0.08	37	0.36	34	0.45
1	38	0.35	32	0.54	29	0.62
2	42	0.20	40	0.29	30	0.61
3	45	0.08	43	0.16	38	0.35

c) ARIMA, Final_model

Model	RMSE	R2
ARIMA(1,0,0)	35	0.46
ARIMA(0,1,0)	34	0.49
CRU Final_model	24	0.74

d)

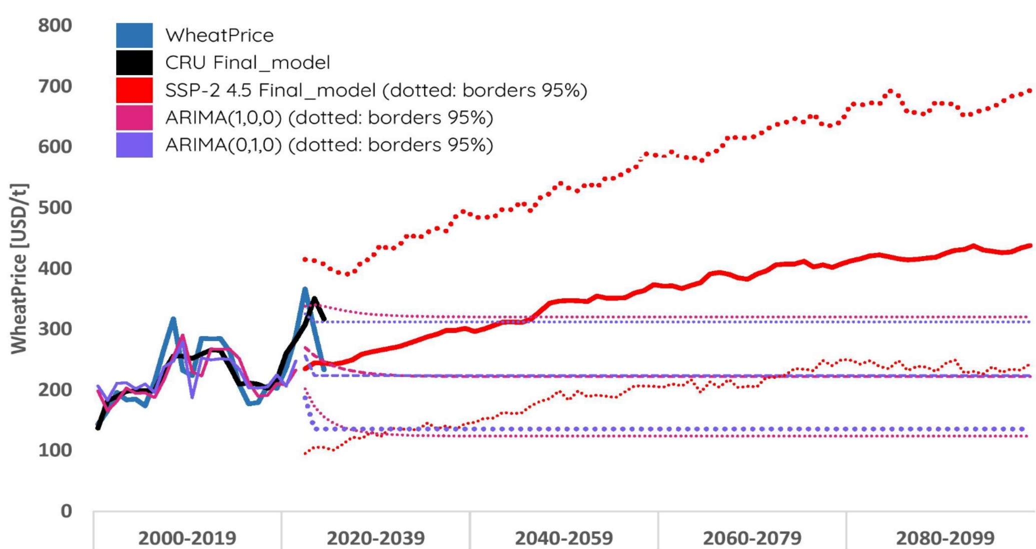

Fig. S4. Matrixes of all tested models SWS over arable land (a) and SWS over wheat producing area of 10 largest wheat exporters (b) vs. World Bank wheat price (USD/t). The yellow marked combinations were used for the final model (the ensemble of 4 best performing models called Final model). At (c) the performance of benchmark ARIMA based models with the Final_model is shown. The annually resolved reported wheat prices and their estimates by 4 different approaches for (2000-2021) and the model projections till 2100 are shown for comparison at Fig (d).

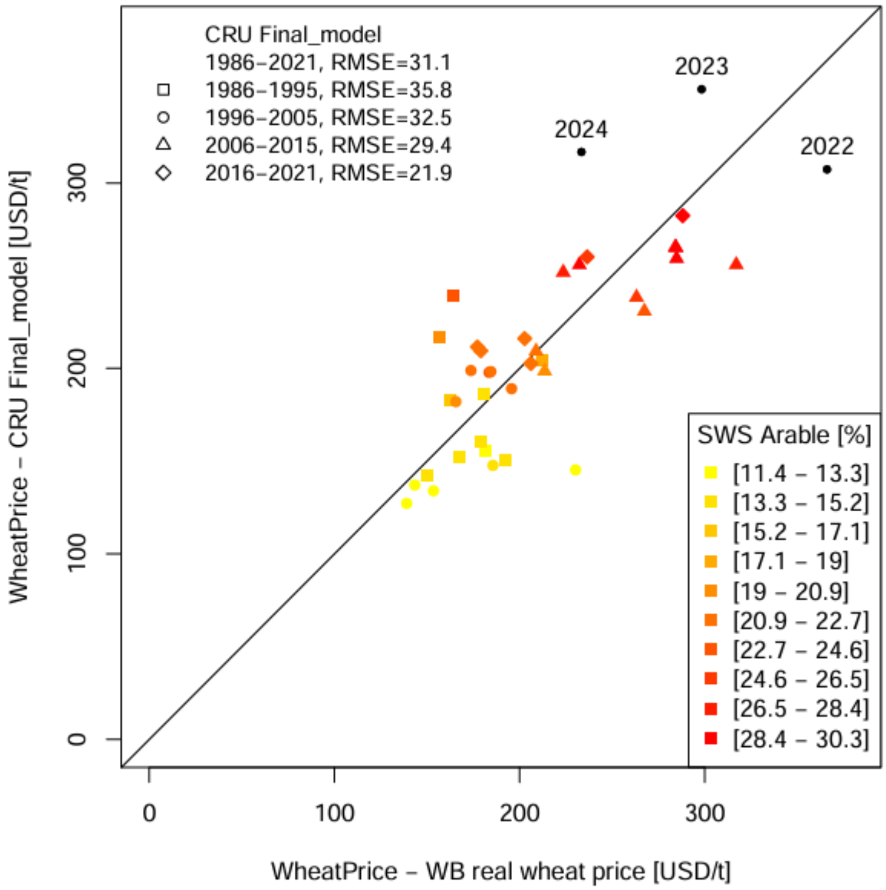

Fig. S5. Wheat price based on the World Bank prices and price estimated using Final_model and observed CRU data modelled for period 1986-2024 ($R^2 = 0.62$) with the RMSE of the model estimates provided for 4 periods and the entire 38 years. The model has been developed only using data for period 2001-2021 ($R^2 = 0.74$) with color depicting the area of the World affected by SWS. Applying the final model for the years 1986-1999 & 2022-2024 for which it has not been trained resulted in $R^2 = 0.55$.

a)

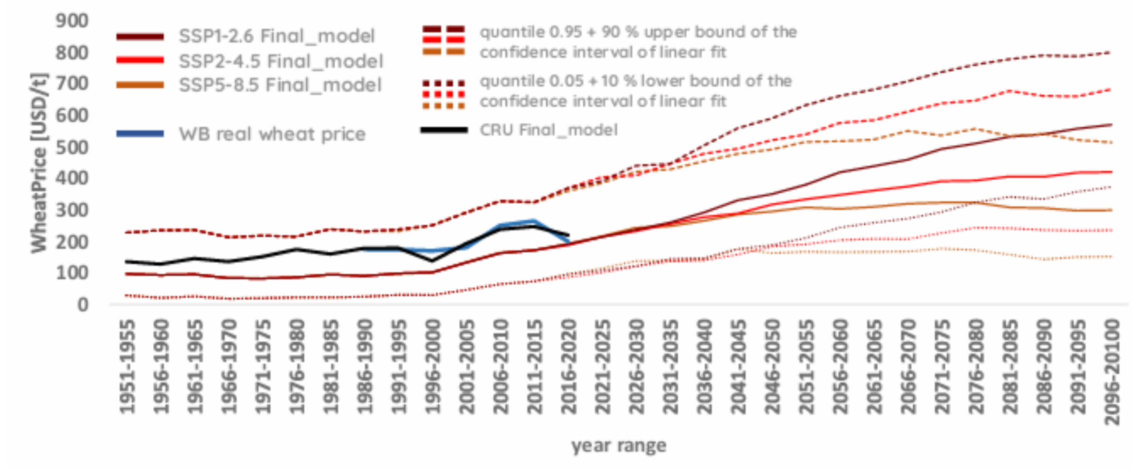

b)

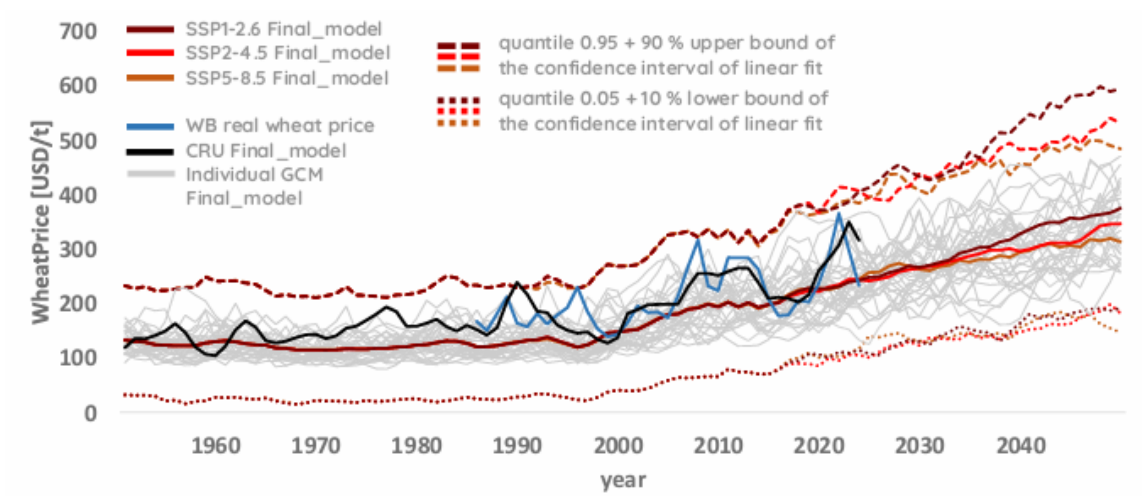

Fig. S6. a) Time series of the reported (blue) and estimated wheat price values via the Final_mocel for the 2000–2024 period using as climate inputs both observed CRU data (black) and for CMIP6 GCM model ensemble (red tones) median (solid line) and 5th and 95th quantile for the entire 21st century. The price values are expressed as 5-year averages; b) The same as (a) but only for the period 1951-2050 for annual values as well as estimates of all 31 individual GCM runs for each SSP.

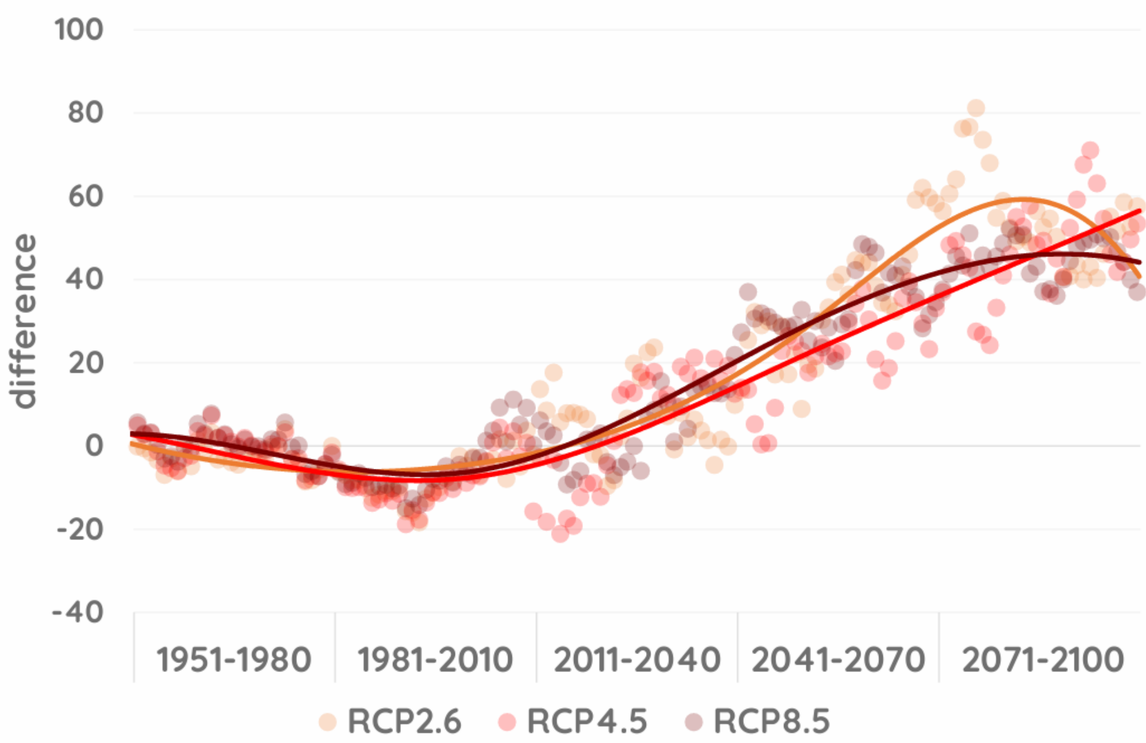

Fig. S7. Comparison of the relative difference in the wheat prices based on the CMIP6_Final model and CMIP5_Final model ensembles. The difference between the mean annual prices indicate slightly higher growth of prices toward the end of the 21[st] century under CMIP6 ensemble runs.

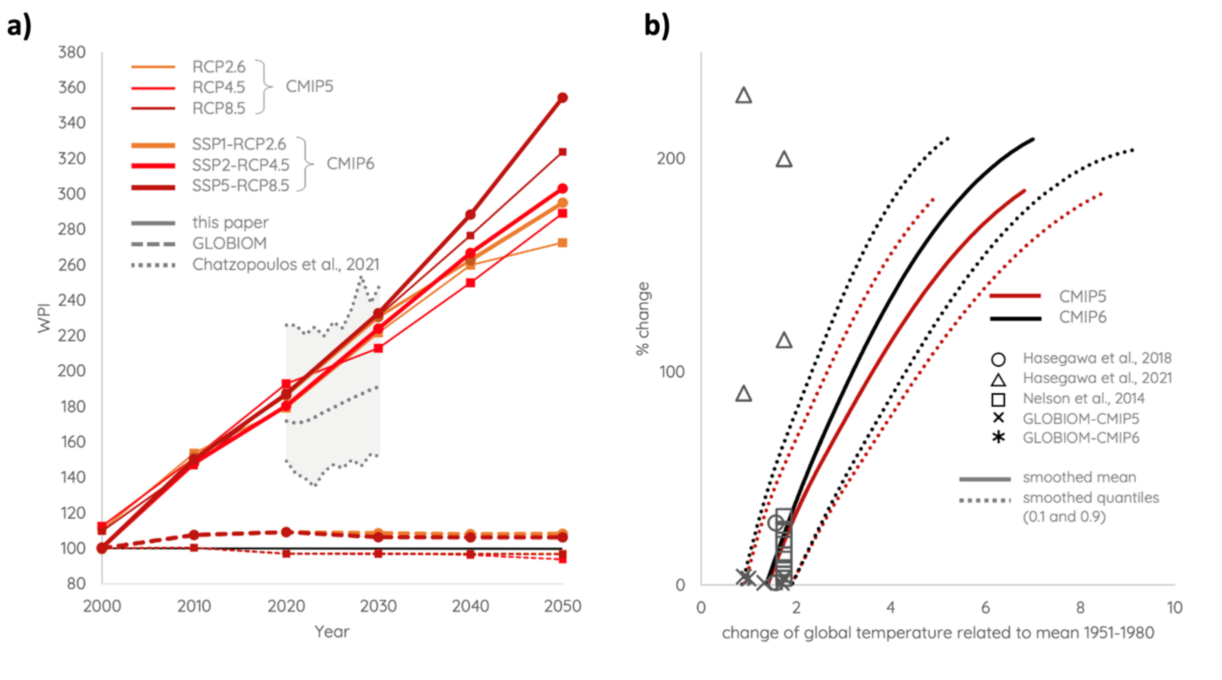

Fig. S8. Comparison of the literature on the wheat price index. a) WPI values estimated by climate change scenarios for CMIP5 and CMIP6 in this paper, Global Biosphere Management Model (GLOBIOM) data vs. the literature between 2000 and 2050. b) Percentage of change in the WPI related to the baseline of this study and the literature for the different levels of global warming (change of global temperature related to mean 1951 - 1980)

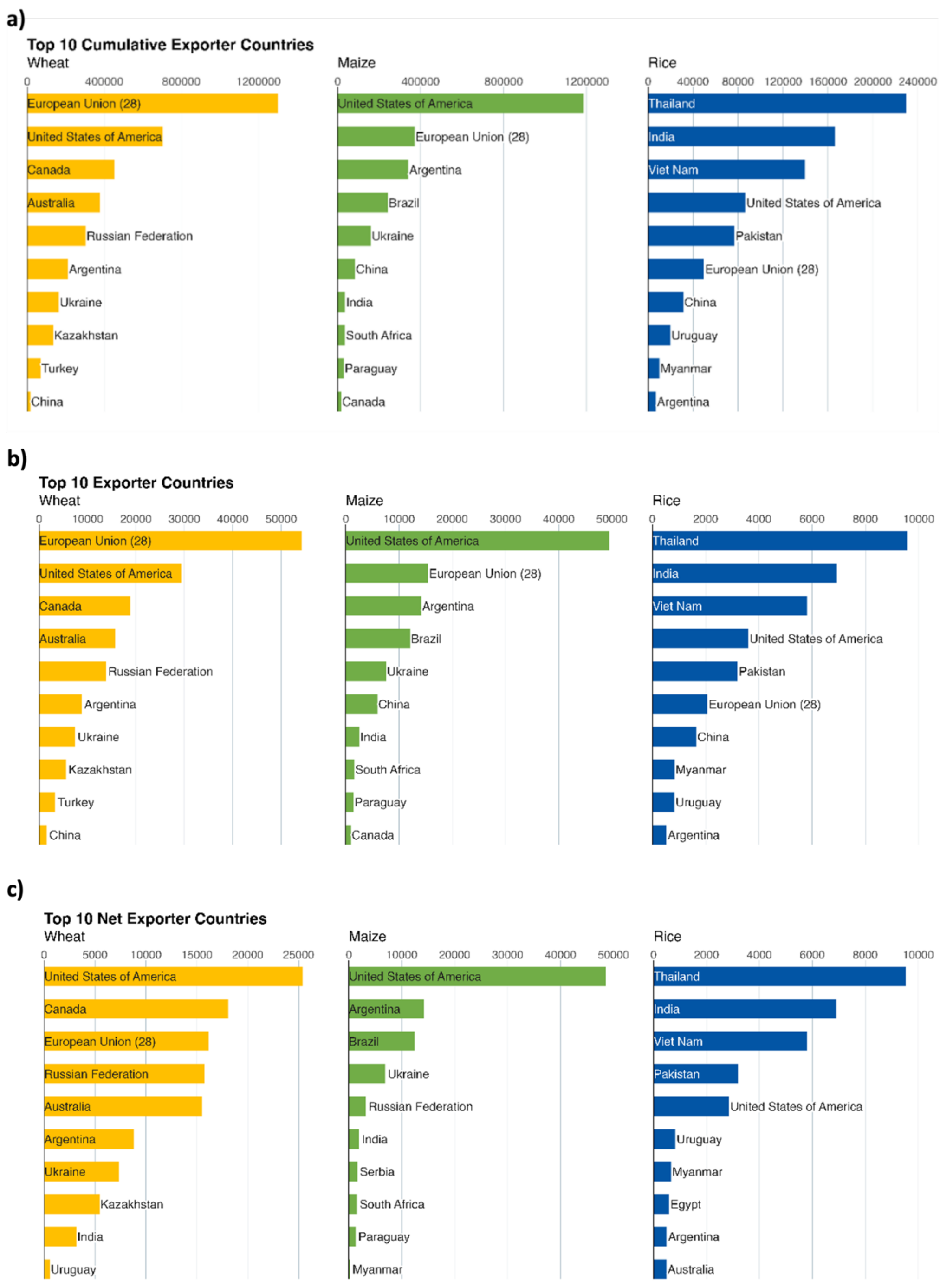

Fig. S9. Top 10 key player countries in the wheat, maize and rice market between 2000 and 2019 from FAOSTAT. a) Top 10 cumulative exporter countries: sum of total export quantities between 2000 and 2019. b) Top 10 exporter countries: mean of the total export quantities between 2000 and 2019. c) Top 10 net exporter countries: mean of the total export minus total import quantities between 2000 and 2019.

Table S1. Definitions of severe water scarcity (SWS) used. All conditions must be fulfilled for the evaluated climate grid cell to be categorized as experiencing severe or extreme water scarcity during a given year. The sensitive period (SP) was defined as the four months prior to the harvest of a particular crop. The standardized precipitation evapotranspiration index (SPEI) is employed as it encodes the imbalance between precipitation and potential evapotranspiration. This imbalance captures the duration and severity of a drought event from hydroclimatic variables at large (i.e. climate grid) scales.

	Description
SPEI: 1 month *Indicating intensive short-term anomaly*	SPEI-1 is lower than -2.0 for at least one month during SP
SPEI: 3 months *Indicating an unusually dry growing season*	SPEI-3 is lower than 0 for at least 3 months in during the SP and in the same time lower than -2.0 for at least one month during SP
SPEI: 12 months *Indicating a long-term water anomaly*	SPEI-12 is lower than 0 for at least 3 months during the SP and in the same time lower than -1.5 for at least one month during the SP

Table S2. Overview of the best performing linear models for estimating the World Bank wheat price (USD/t) based on the area affected by severe water scarcity. The aggregated values indicate the combined performance of the models as the ensemble is expanded by adding additional models to Model_1.

Name	Full name of model	RMSE	Coefficient of determination	Aggregated RMSE	Aggregated coefficient of determination	Model parameters	Weight in the final model
Model_1	SWS_Arable_window3_lag2	26.8	0.68	26.8	0.68	Y=9.2891X-0.1869	0.3564
Model_2	SWS_WhA10Ex_window3_lag1	29.0	0.62	24.7	0.73	Y=5.0611X+122.7179	0.2871
Model_3	SWS_Arable_window2_lag1	29.2	0.62	24.7	0.73	Y=10.5442X+28.7423	0.1782
Model_4	SWS_WhA10Ex_window3_lag2	29.5	0.61	24.3	0.74	Y=4.7310X+134.8245	0.1782

Table S3. Overview of the CMIP6 global circulation models (GCMs) used in this study (with brief descriptions). The historical run (i.e., 1850–2014) and the runs of three future emissions scenarios (i.e., SSP1-2.6, SSP2-4.5 and SSP5-8.5; 2015–2100) are used from each model. "*" indicates that the simulations under all three future SSPs are available. Otherwise, only SSP2-4.5 and SSP5-8.5 are available. The first ensemble run is used if a model is associated with multiple ensemble runs.

	Model name	Resolution (long. by lat.)	Origin
1*	ACCESS-CM2	1.875×1.250	Commonwealth Scientific and Industrial Research Organization, Australia
2*	ACCESS-ESM1-5	1.875×1.250	Commonwealth Scientific and Industrial Research Organization, Australia
3*	AWI-CM-1-1-MR	0.938 × 0.935	Alfred Wegener Institute, Germany
4*	BCC-CSM2-MR	1.125 × 1.121	Beijing Climate Center, China
5*	CanESM5	2.813×2.789	Canadian Centre for Climate Modeling and Analysis, Canada
6*	CanESM5-CanOE	2.813×2.789	Canadian Centre for Climate Modeling and Analysis, Canada
7*	CAS-ESM2-0	1.406×1.417	Chinese Academy of Sciences, China
8*	CESM2-WACCM	1.250×0.942	National Center for Atmospheric Research, USA
9*	CMCC-CM2-SR5	1.250×0.942	Centro Euro-Mediterraneo sui Cambiamenti Climatici, Italy
10*	CMCC-ESM2	1.250×0.942	Centro Euro-Mediterraneo sui Cambiamenti Climatici, Italy
11*	EC-Earth3	0.703×0.702	EC-Earth Consortium, Europe
12	EC-Earth3-CC	0.703×0.702	EC-Earth Consortium, Europe
13*	FGOALS-f3-L	1.250×1.000	Chinese Academy of Sciences, China
14*	FGOALS-g3	2.000×2.084	Chinese Academy of Sciences, China
15*	GFDL-ESM4	1.250×1.000	Geophysical Fluid Dynamics Laboratory, USA
16*	GISS-E2-1-G	2.500×2.000	NASA GISS, USA
17*	HadGEM3-GC31-LL	1.875×1.250	Met Office Hadley Centre, UK
18*	INM-CM4-8	2.000×1.500	Institute for Numerical Mathematics, Russia
19*	INM-CM5-0	2.000×1.500	Institute for Numerical Mathematics, Russia
20*	IPSL-CM6A-LR	2.500×1.268	Institut Pierre Simon Laplace, France
21*	KACE-1-0-G	1.875×1.250	Korea Meteorological Administration, Korea
22*	KIOST-ESM	1.875×1.895	Korea Institute of Ocean Science and Technology, Korea
23*	MIROC-ES2L	2.813×2.789	The University of Tokyo, Japan
24*	MIROC6	1.406×1.401	The University of Tokyo, Japan
25*	MPI-ESM1-2-HR	0.938×0.935	Max Planck Institute for Meteorology, Germany
26*	MPI-ESM1-2-LR	1.875×1.865	Max Planck Institute for Meteorology, Germany
27*	MRI-ESM2-0	1.125×1.121	Meteorological Research Institute, Japan
28*	NorESM2-LM	2.500×1.895	Norwegian Climate Center, Norway
29*	NorESM2-MM	1.250×0.942	Norwegian Climate Center, Norway
30*	TaiESM1	1.250×0.942	Academia Sinica, Taiwan
31*	UKESM1-0-LL	1.875×1.250	Met Office Hadley Centre, UK

Table S4. List of the CMIP5 global circulation models (GCMs) used in this study with brief descriptions. The historical run (i.e., 1850–2005) and the runs of three future emissions scenarios (i.e., RCP2.6, RCP4.5 and RCP8.5; 2006–2100) are used from each model. "*" indicates that the simulations under all three future RCPs are available. Otherwise, only RCP4.5 and RCP8.5 are available. The first ensemble run is used if a model is associated with multiple ensemble runs.

	Model name	Resolution (long. by lat.)	Origin
1*	BCC-CSM1.1	2.815 × 2.815	Beijing Climate Center, China
2*	CanESM2	2.815 × 2.815	Canadian Centre for Climate, Canada
3*	CCSM4	1.25 × 0.9	National Center for Atmospheric Research, USA
4	CESM1-BGC	1.25 × 0.9	National Center for Atmospheric Research, USA
5*	CESM1-CAM5	1.25 × 0.9	National Center for Atmospheric Research, USA
6	CMCC-CM	0.75 × 0.75	Centro Euro-Mediterraneo per i Cambiamenti, Italy
7	CMCC-CMS	1.875 × 1.875	Centro Euro-Mediterraneo per i Cambiamenti, Italy
8*	CNRM-CM5	1.40 × 1.40	Centre National de Recherches Meteorologiques, France
9*	CSIRO-Mk3.6	1.875 × 1.875	Commonwealth Scientific and Industrial Research, Australia
10*	FGOALS-g2	2.815 × 3.0	Institute of Atmospheric Physics, CAS, China
11*	GFDL-CM3	2.5 × 2.0	Geophysical Fluid Dynamics Laboratory, USA
12*	GFDL-ESM2G	2.5 × 2.0	Geophysical Fluid Dynamics Laboratory, USA
13*	GFDL-ESM2 M	2.5 × 2.0	Geophysical Fluid Dynamics Laboratory, USA
14*	GISS-E2-H	2.5 × 2.0	NASA Goddard Institute for Space Studies, USA
15*	GISS-E2-R	2.5 × 2.0	NASA Goddard Institute for Space Studies, USA
16	HadGEM2-CC	1.875 × 1.25	Met Office Hadley Centre, UK
17*	HadGEM2-ES	1.875 × 1.25	Met Office Hadley Centre, UK
18	INM-CM4	2.0 × 1.5	Institute for Numerical Mathematics, Russia
19*	IPSL-CM5A-LR	3.75 × 1.875	Institut Pierre-Simon Laplace, France
20*	IPSL-CM5A-MR	2.5 × 1.25	Institut Pierre-Simon Laplace, France
21	IPSL-CM5B-LR	3.75 × 1.875	Institut Pierre-Simon Laplace, France
22*	MIROC5	1.40 × 1.40	Atmosphere and Ocean Research Institute, Japan
23*	MIROC-ESM	2.815 × 2.815	Japan Agency for Marine-Earth Science and Technology, Japan
24*	MIROC-ESM-CHEM	2.815 × 2.815	Japan Agency for Marine-Earth Science and Technology, Japan
25*	MPI-ESM-LR	1.875 × 1.875	Max Planck Institute for Meteorology, Germany
26*	MRI-CGCM3	1.125 × 1.125	Meteorological Research Institute, Japan
27	NorESM1-M	2.5 × 1.875	Norwegian Climate Centre, Norway